

Cosmic Shear from STIS Pure Parallels

II Analysis

H. Hämmerle^{1,2}, J.-M. Miralles³, P. Schneider^{1,2}, T. Erben^{2,4,5},
 R. A. E. Fosbury³, W. Freudling³, N. Pirzkal³, B. Jain⁶,
 S. D. M. White²

¹Institut für Astrophysik und Extraterrestrische Forschung der Universität Bonn, Auf dem
 Hügel 71, D-53121 Bonn, Germany

²Max-Planck-Institut für Astrophysik, Karl-Schwarzschild Str. 1, D-85748 Garching, Germany

³ST-ECF, Karl-Schwarzschild Str. 2, D-85748 Garching, Germany

⁴Institut d'Astrophysique de Paris, 98bis Boulevard Arago, F-75014 Paris, France

⁵Observatoire de Paris, DEMIRM 61, Avenue de l'Observatoire, F-75014 Paris, France

⁶Department of Physics and Astronomy, University of Pennsylvania 209 S. 33rd Street,
 Philadelphia, PA 19104 USA

1 Cosmic Shear

The measurement of cosmic shear requires deep imaging (to beat the noise due to the galaxies' intrinsic ellipticity distribution) with high image quality (because every non-corrected PSF anisotropy mimics cosmic shear) on many lines of sight to sample the statistics of large-scale structure. The STIS camera on-board HST has a very good performance in that respect, which we demonstrate here, by using archival data from the STIS pure parallel program between June 1997 and October 1998. The data reduction and catalog production are described in the poster *Detection of Cosmic Shear From STIS Parallel Archive Data: Data Analysis* presented here and the paper Pirzkal et al. (2001).

2 STIS: PSF correction

The expected distortion of galaxy images by cosmic shear on the angular scale of STIS ($\sim 50''$) is a few percent, therefore the PSF anisotropy has to be understood and controlled to an accuracy of better than 1%. In Fig. 1 we show that the mean ellipticity of stars are small and can be considered constant at the one sigma level.

In addition to the variations from field to field, we find a spatial variation of the PSF within individual fields, as shown in Fig. 3, to which we fitted a second-order polynomial as a function of position on the CCD. We also find some very short timescale variations of the PSF (also shown in Fig. 3) which are likely due to breathing of the telescope.

In Fig. 2 we show that the PSF anisotropy corrections are very small, they change the mean of the galaxy ellipticities on a field only slightly. We also checked the effect of the anisotropy correction on the cosmic shear result and find that it does not change noticeably.

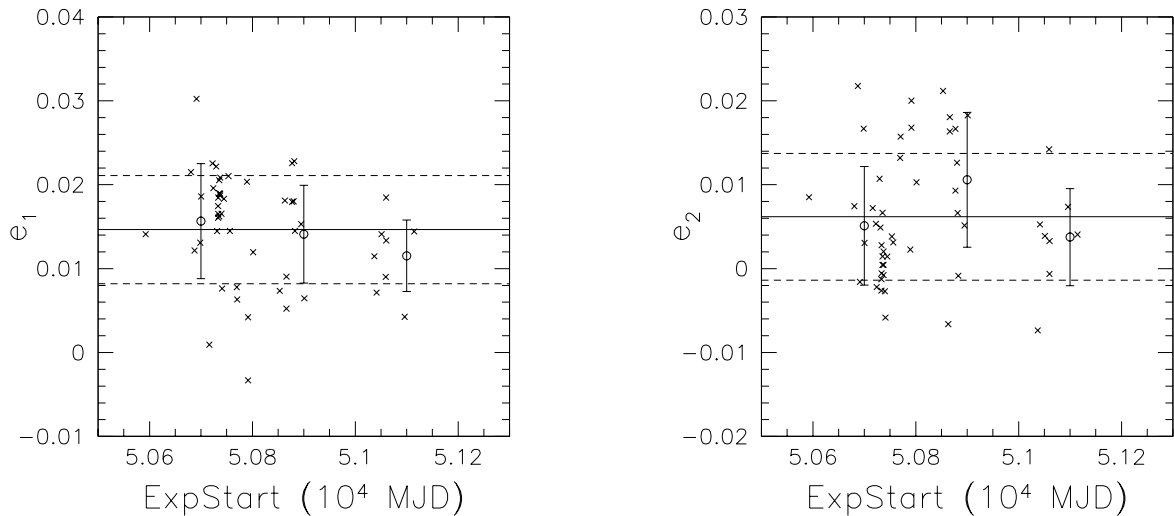


Figure 1: Mean of the ellipticity e_1 (left) and e_2 (right) of the star fields vs. exposure start time (Modified Julian Date). Both components can be approximated by a constant over the time period covered. The straight lines show the mean over all the fields, the dashed lines are the corresponding 1σ errors. The circles denote the mean over stars in bins between 5.06×10^4 , 5.08×10^4 , 5.10×10^4 , 5.12×10^4 (MJD) with the corresponding 1σ error bars.

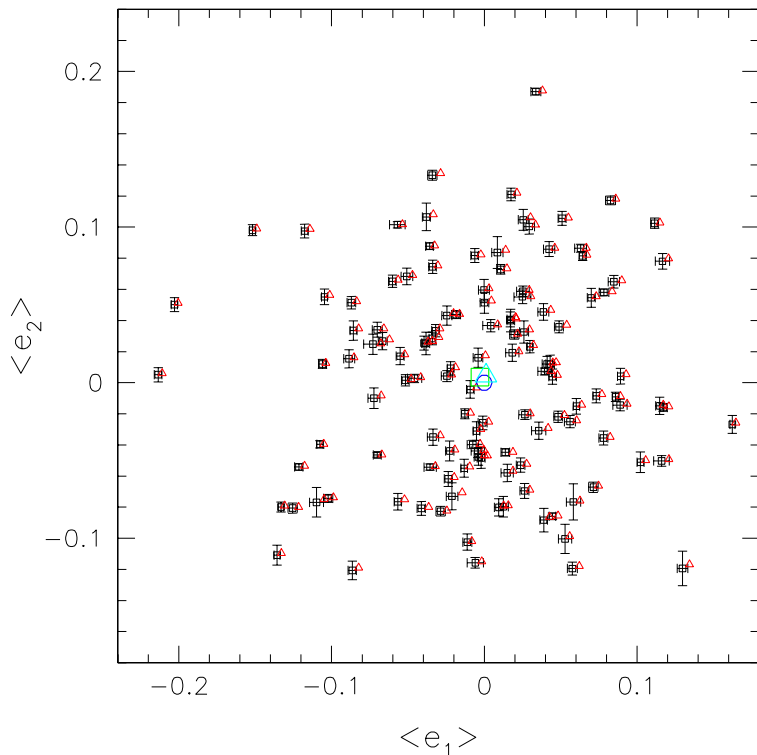


Figure 2: For 121 galaxy fields we plot the mean uncorrected ellipticity of galaxies (triangles) as well as the mean corrected ellipticity (squares). The error bars attached to the squares denote 3 times the dispersion of the field-averaged corrected ellipticities when the different PSF model fits are used. The shift of the corrected mean ellipticities towards negative e_1 is expected from the behaviour of the stellar ellipticities plotted in Fig. 1. The red triangle and cyan square in the center denote the mean over all galaxy fields of the uncorrected and corrected mean ellipticities, respectively; the size of the symbols show the 1σ errors on the mean. The circle shows the origin for reference. The mean is compatible with zero.

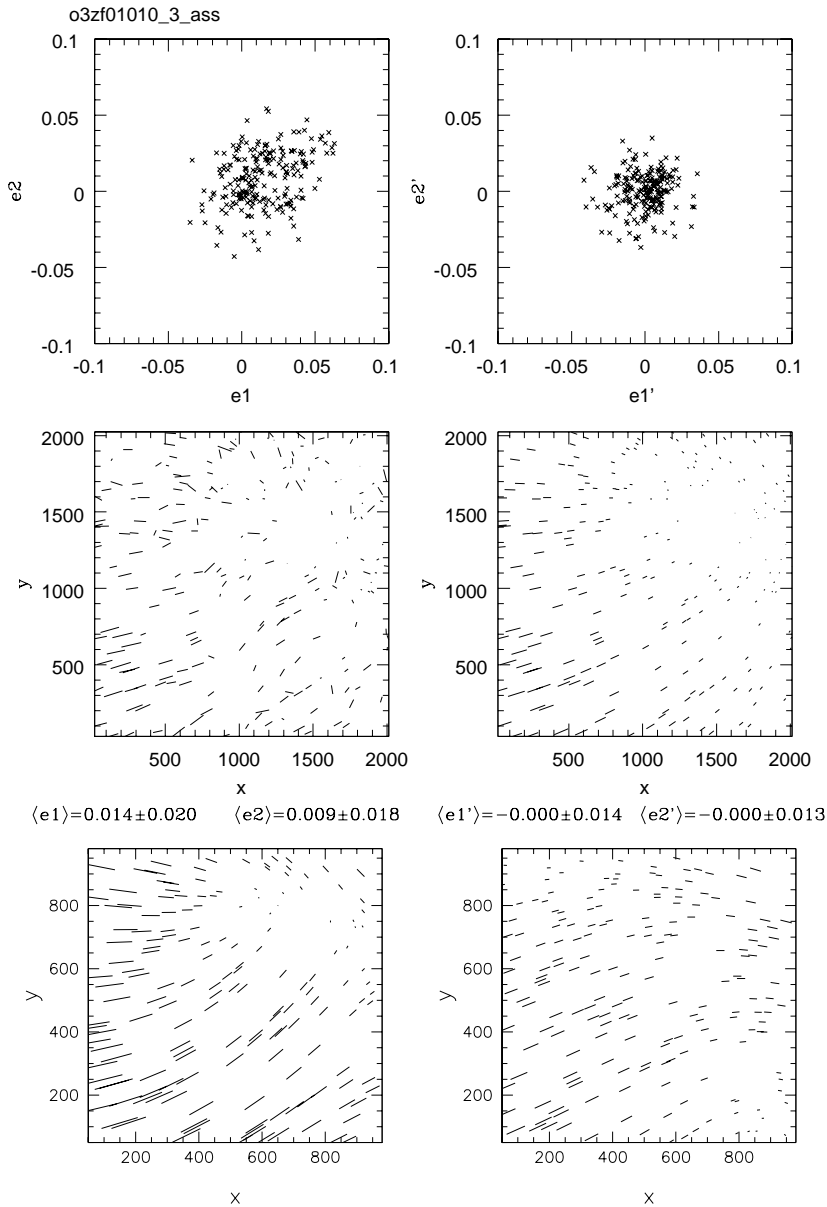


Figure 3: For one of the star fields the distribution of the ellipticities of stars are shown before (top left) and after (top right) correcting for PSF anisotropy. The middle left panel shows the spatial distribution of the ellipticities across the STIS field, the middle right the fitted second order polynomial at the star positions. The length of the sticks indicates the modulus of the ellipticity, the orientation gives the position angle. For individual exposures of this field, which were taken with a time difference of only 30 minutes we show the values of the polynomials for the anisotropy correction in the lower panels. One clearly sees the short timescale variations which are likely due to breathing of the telescope.

3 Results

We analysed the ellipticities of galaxies in 121 galaxy fields, which were corrected for PSF effects using 21 measured PSFs from low galactic latitude fields (star fields). The quantity estimated was the shear dispersion in each field. We apply a weighting to individual galaxies according to the weighting scheme in Erben et al. (2001). By randomizing the orientations of the galaxy images, we obtain probability distributions for our estimator in the absence of shear, which are shown in Fig. 3, with and without applying the weighting; this serves as an estimate of the significance of our result.

In Fig. 5 we compare our result for the cosmic shear with weighting individual galaxies to those obtained for larger scales by other groups.

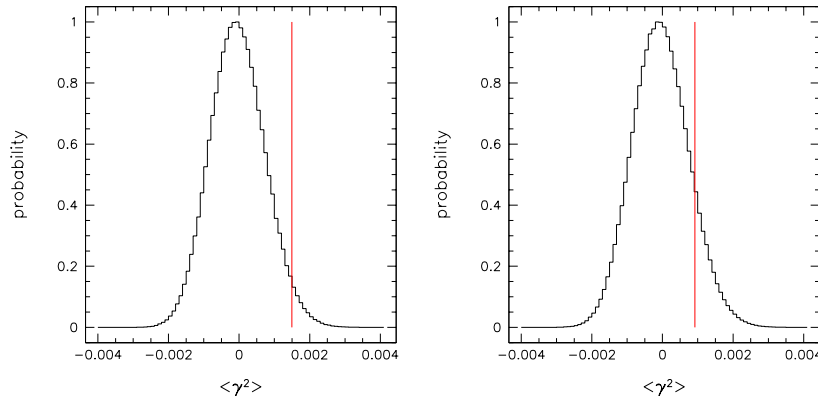


Figure 4: Probability distribution of the cosmic shear dispersion estimator calculated from the data by randomizing the orientations of galaxies. The vertical line indicates the actually measured value; left is with, right without weighting the galaxies depending on their noise level.

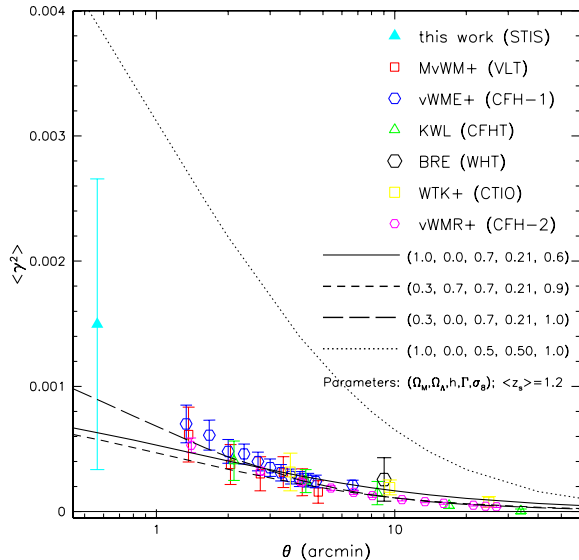


Figure 5: Comparison of our cosmic shear result (big triangle at $0.5'$) with measurements at larger angular scales and with model predictions. The lines show the theoretical predictions if one uses different cosmological models, where we indicate Ω_m , Ω_Λ , h , Γ and σ_8 . The redshift distribution was taken from Brainerd et al. (1996) with a mean source redshift of $\langle z_s \rangle = 1.2$. Given the different galaxy selection implied by our STIS data, which may imply a substantially different redshift distribution from that obtained from ground-based observations, the apparent discrepancy may be due to a higher mean redshift.

References

- Bacon, D., Refregier, A., Ellis, R.S., 2000, MNRAS, 318, 625
- Brainerd, T.G., Blandford, R.D., Smail, I., 1996, ApJ, 466, 623
- Erben, T., van Waerbeke, L., Bertin, E., Mellier, Y., Schneider, P., 2001, A&A, 366, 717
- Kaiser, N., Wilson, G., Luppino, G.A., 2000, submitted to ApJ, astro-ph/0003338
- Maoli, R., Mellier, Y., van Waerbeke, L., Schneider, P., Jain, B., Bernardeau, F., Erben, T., Fort, B., 2001, A&A, 368, 766
- Pirzkal, N., Collodel, L., Erben, T., Fosbury, R.A.E., Freudling, W., Hämmerle, H., Jain, B., Micol, A., Miralles, J.-M., Schneider, P., Seitz, S., White, S.D.M., 2001, A&A in press, astro-ph/0102330
- van Waerbeke, L., Mellier, Y., Erben, T., Cuillandre, J.C., Bernardeau, F., Maoli, R., Bertin, E., Mc Cracken, H.J., Le Fèvre, O., Fort, B., Dantel-Fort, M., Jain, B., Schneider, P., 2000, A&A, 358, 30
- van Waerbeke, L., Mellier, Y., Radovich, M., Bertin, E., Dantel-Fort, M., Mc Cracken, H.J., Le Fèvre, O., Foucaud, S., Cuillandre, J.C., Erben, T., Jain, B., Schneider, P., Bernardeau, F., Fort, B., 2001, A&A in press, astro-ph/0101511
- Wittman, D.M., Tyson, J.A., Kirkman, D., Dell'Antonio, I., Bernstein, G., 2000, Nature, 405, 143